Modelling and Control of a Car's Longitudinal Dynamics

João Fonseca-93094 joao.r.fonseca@tecnico.ulisboa.pt
Teresa Fernandes-93183 teresa.fernandes@tecnico.ulisboa.pt

Instituto Superior Técnico, Lisboa, Portugal

January 2023

Abstract

System modelling is, and has always been, of most importance in the robotics field, as every robot requires a model to be controlled and to fulfil its functionality. The study of autonomous vehicles is a sub-field of robotics that has acquired a substantial amount of attention in the past few years, being labelled as the future of driving technology. This paper shows a thorough modelling study of a vehicle's longitudinal dynamics as well as its control.
Keywords: Robotics, Car Modeeling, Autonomous Vehicles, Control

1. Introduction

The study of autonomous cars, is of great importance for the robotics field. It has the potential to bring significant changes in our society, such as an increase in road safety or automation of transportation tasks for example.

2. Car Model

Being a well known important area in robotics, there are many possibilities for the car model. In this paper we will focus on the longitudinal dynamics [1]. A force balance along the vehicle's longitudinal axis yields

$$m\ddot{x} = F_{xr} + F_{xf} - F_{aero} - R_{xf} - R_{xr}, \quad (1)$$

where the car is assumed to move only on the XY plane, F_{xr} is the longitudinal tire force at the rear tires, F_{xf} is the longitudinal tire force at the front tires, F_{aero} is the equivalent longitudinal aerodynamic drag force and R_{xf} and R_{xr} are the forces due to rolling resistance at the front and rear tires respectively.

2.1. Aerodynamic Drag Force

The equivalent aerodynamic drag force on a vehicle can be represented as

$$F_{aero} = \frac{1}{2}\rho C_d A_F (\dot{x} + V_{wind})^2, \quad (2)$$

where ρ is the air mass density, C_d is the aerodynamic drag coefficient, A_F the projected area of the vehicle in the direction of movement and V_{wind} is the wind's velocity (positive for headwind, negative otherwise).

C_d and R_x can be roughly determined from a coast-down test [2],

$$\begin{cases} C_d = \frac{2m\beta \tan^{-1}\beta}{V_o T \rho A_F} \\ R_x = \frac{V_o m \tan^{-1}\beta}{\beta T} \end{cases}, \quad (3)$$

where V_o is the known initial longitudinal velocity and T the total time for the vehicle to coast-down to a stop and β obtained by solving

$$\dot{x} = \frac{V_o}{\beta} \tan\left[\left(1 - \frac{1}{T}\right)\tan^{-1}\beta\right], \quad (4)$$

using measurements of t and $\dot{x}$.

2.2. Longitudinal Tire Forces

These forces are caused due to friction from the ground acting on the tires. Experimental results established that these depend on the slip ratio, the normal load on the tire and the friction coefficient of the tire-road interface.

We start by defining the longitudinal slip ratio as

$$\begin{cases} \sigma_x = \frac{r_{eff}\omega_w - \dot{x}}{\dot{x}} \text{ during braking} \\ \sigma_x = \frac{r_{eff}\omega_w - \dot{x}}{r_{eff}\omega_w} \text{ during acceleration} \end{cases}, \quad (5)$$

where ω_w is the rotational speed of the wheel, and r_{eff} is the effective radius of the tires, *i.e.*, the radius which relates ω_w to the linear longitudinal velocity of the wheel: $V_{eff} = r_{eff}\omega_w$. r_{eff} can be obtained as a function of the undeformed radius r_w and the radius with deformation r_{stat} as

$$r_{eff} = \frac{sin^{-1}\left[cos^{-1}(r_{stat}/r_w)\right]}{cos^{-1}(r_{stat}/r_w)} \cdot r_w \quad (6)$$

In the cases where this longitudinal slip ratio is small (dry surfaces), the tire force has an approximate linear relation with the slip ratio

$$\begin{cases} F_{xf} = C_{\sigma xf}\sigma_{xf} \\ F_{xr} = C_{\sigma xr}\sigma_{xr} \end{cases}, \tag{7}$$

where $C_{\sigma ft}$ and $C_{\sigma rt}$ are the longitudinal tire stiffness parameters of the front and rear tires respectively, and σ_{xf} and σ_{xr} are calculated using the torational speed of the front and rear wheels respectively.

2.3. Rolling Resistance

The tire and the road are both vulnerable to deformation as the tire rotates. The road is much stiffer, which makes its deformation negligible. However, the tire is elastic and thus the energy spent in deforming the tire material is not completely recovered when the material returns to its original shape. This can be modelled as a force on the tires called the rolling resistance that acts to oppose the motion of the vehicle, mathematically written as

$$R_{xf} + R_{xr} = f(F_{zf} + F_{zr}), \tag{8}$$

where f is the rolling resistance coefficient and F_{zr} and F_{zf} are the normal tire forces.

2.3.1 Normal Tire Forces

In addition to the total weight of the vehicle, the normal load on the tires is also influenced by aerodynamic drag forces and longitudinal acceleration. Manipulating the moments in the contact points of the rear and front tires we get

$$\begin{cases} F_{zf} = \frac{-F_{aero}h_{aeroo} - m\ddot{x}h + mgl_f}{l_f + l_r} \\ F_{zr} = \frac{F_{aero}h_{aeroo} + m\ddot{x}h + mgl_f}{l_f + l_r} \end{cases}, \tag{9}$$

where l_f and l_r are the longitudinal distances from the front and rear axles from the centre of gravity (c.g) of the car, h is the height of the c.g to the surface and h_{aero} is the height of the location at which the equivalent aerodynamic force acts.

2.4. Driveline Dynamics

The longitudinal tire forces on the motion equation 1, F_{xr} and F_{xf} are the main forces that allow the car to move forward. These not only depend on the car's longitudinal velocity $\dot{x}$ but also are highly influenced by the rotational wheel velocity ω_w, which is highly affected by the driveline dynamics (Figure 1).

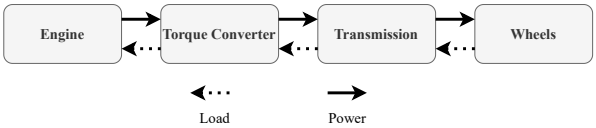

Figure 1: Driveline components.

2.4.1 Engine

The engine rotational speed dynamics can be described by

$$I_e\dot{\omega}_e = T_e - T_p, \tag{10}$$

where T_e is the net engine torque due to combustion after frictional and accessory losses. This torque depends on the acceleration input from the car driver. T_e can eb obtained from two ways: a complex mathematical model that accounts for the engine's manifold pressure balance, or an engine map obtained from experimental data, *i.e.*, an experimental function $T_e(\omega_e, p_{man})$, where p_{man} is the engine's manifold pressure. T_p is obtained from the equations that model the torque converter block, namely 11 and 12, described in the next section.

2.4.2 Torque Converter

A torque converter is a type of fluid coupling component that transfers rotating power from a prime mover, like an internal combustion engine, to a rotating driven load. Its major components are a pump, a turbine and the transmission fluid.

The following torque converter model, based on [3], assumes SI units and is useful due to its simplicity. If the operating point is in converter mode ($\omega_t/\omega_p < 0.9$) the equations are

$$\begin{cases} T_p = 3.4325 - 3\omega_p^2 + 2.2210 \times 10^{-3}\omega_p\omega_t \\ -4.6041 \times 10^{-3}\omega_t^2 \\ \\ T_t = 5.7656 \times 10^{-3}\omega_p^2 + 0.3107 \times 10^{-3}\omega_p\omega_t \\ -5.4323 \times 10^{-3}\omega_t^2 \end{cases}, \tag{11}$$

where T_p and T_t are pump and turbine torques and ω_p, ω_t are the correspondent rotation speeds.

If, on the other hand, the converter is in fluid coupling mode ($\omega_t/\omega_p \geq 0.9$), the equations become

$$\begin{cases} T_p = T_t = -6.7644 \times 10^{-3}\omega_p^2 + 32.0024 \times 10^{-3}\omega_p\omega_t \\ -25.2441 \times 10^{-3}\omega_t^2 \end{cases} \tag{12}$$

2.4.3 Transmission Dynamics

The car's behaviour changes based on the current operating gear. Let R be the gear ratio of the transmission, in general $R < 1$ and the higher the gear, the bigger the value of the ratio.

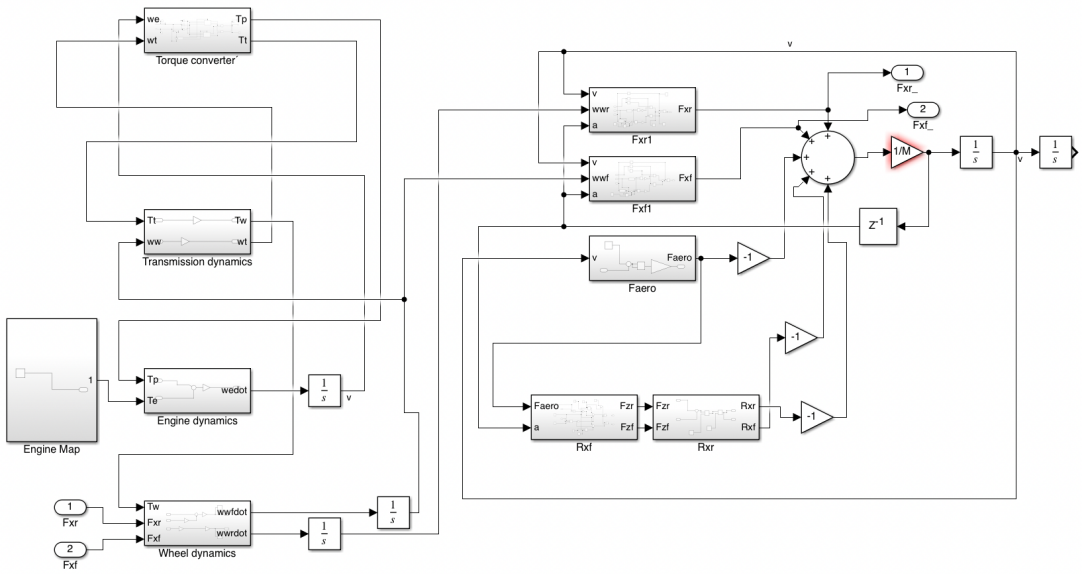

Figure 2: Longitudinal dynamics block diagram.

In a steady-state scenario, the equations relating transmission ω_t and wheel ω_w speeds, as well as turbine torque T_t and wheel torque T_w are written as

$$\begin{cases} T_t = RT_w \\ \omega_w = R\omega_t \end{cases} . \tag{13}$$

During a gear changes, equations very complex and are thoroughly described in [4]. However, a simple first order approximation is

$$\begin{cases} \tau\dot{T}_w + T_w = \frac{1}{R}T_t \\ \tau\dot{\omega}_t + \omega_t = \frac{1}{R}\omega_w \end{cases} , \tag{14}$$

where R is the ratio of new gear to which the transmission shifts and T_w, ω_t are initialised with 0 and $\frac{1}{R_{old}}\omega_w$, where R_{old} is the gear before shift. Gear change is assumed to be complete once these equations converge to the steady-state equations 13.

2.4.4 Wheel Dynamics

Finally, the equation that models rotational dynamics of the driving wheels (assuming a front-wheel driven car) is

$$I_w\dot{\omega}_{wf} = T_w - r_{eff}F_{xf} \tag{15}$$

, where ω_{wf} is the rotational speed of the front wheels, and the remaining variables have already been introduced.

For non-driven rear wheels (ω_{wr}),

$$I_w\dot{\omega}_{wr} = -r_{eff}F_{xr} \tag{16}$$

2.5. Longitudinal Dynamics Full Model

Figure 2 shows the combination of driveline dynamics with the implementation of the car's force balance equation 1. This summarises the described longitudinal dynamics model.

3. Longitudinal Control

3.1. Benefits of Longitudinal Control

The term "longitudinal controller" typically refers to any control system that controls the longitudinal motion of the vehicle, for example, its longitudinal velocity, acceleration, or its longitudinal distance from another preceding vehicle in the same lane. A very common example of this is the standard cruise control system in most cars today.

Another example is adaptive cruise control (ACC), which is an extension of Standard Cruise Control. An ACC-equipped car has a radar that measures the distance to other preceding vehicles on the highway. Depending on the absence or presence of preceding vehicles, the car travels at a user-set speed, or at a speed that maintains a desired spacing from the preceding vehicle.

There are several motivations for the development of longitudinal vehicle control systems, such as the desire to improve driver comfort and convenience, highway safety, and the urge to develop solutions to ease traffic congestion on roads. An ACC system provides enhanced driver comfort and convenience by allowing extended operation of the cruise control option even in the presence of other traffic. This system is expected to contribute towards increased safety on the highways, as statistics show that 90% of accidents are caused by human error [5] Other systems have also been designed with the scope to reduce traffic congestion.

3.2. Cruise Control

In a standard cruise control system, the speed of the vehicle is controlled to a desired value using the throttle control input. The longitudinal control system architecture for the cruise control vehicle is designed with an upper level controller and a lower level controller. The upper level controller deter-

mines the desired acceleration for the car. The lower level controller determines the throttle input required to track the desired acceleration.

3.3. Upper Level Controller

A common controller technique is PI control with speed error as the feedback signal:

$$\ddot{x}_{des}(t) = -k_p(V_x - V_{ref}) - k_I \int_0^t (V_x - V_{ref})\, dt \quad (17)$$

with V_{ref} being the desired speed of the user.

If we define the reference position x_{des} as the position of an imagined reference vehicle that is traveling at the reference or desired speed with the following formula:

$$x_{des} = \int_0^t (V_{ref})\, d\tau \quad (18)$$

then we can rewrite the controller as:

$$\ddot{x}_{des} = -k_p(\dot{x} - \dot{x}_{des}) - k_I(x - x_{des}) \quad (19)$$

which is equivalent to spacing control between two vehicles, with $x - x_{des}$ being the space from an imaginary vehicle going at the desired reference speed.

Considering a closed-loop system, the plant model for the control is:

$$P(s) = \frac{1}{s(s\tau + 1)} \quad (20)$$

Then the PI controller is:

$$C(s) = k_p + \frac{k_i}{s} \quad (21)$$

So the closed-loop transfer function is:

$$\frac{V_x}{V_{ref}} = \frac{PC}{1 + PC} = \frac{k_p s + k_i}{\tau s^3 + s^2 + k_p s + k_i} \quad (22)$$

3.3.1 Stability of PI Controller

A root locus of the feedback system is shown in Figure 3 for $K_p = 0.75$, with the ratio $\frac{K_p}{K_i}$ fixed at 4. A value of τ = 0.5 was assumed for the system lag. It can be understood that the closed system is stable for all non-zero K_p. There is one closed-loop real pole and a pair of complex conjugate poles. For a value of K_p= 0.75, the complex poles have a damping ratio of 0.87. If the value of K_p, is increased further beyond 0.75, the damping ratio of the complex poles decreases, and the system becomes less damped.

The Bode magnitude plot of the closed-loop transfer function is shown in Figure 4 for a value of K_p = 0.75. As seen in the figure, the resulting bandwidth of the closed-loop system is 0.2 Hz.

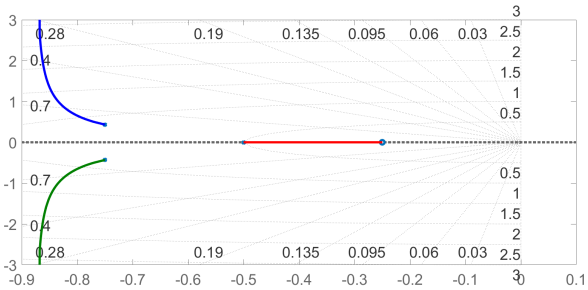

Figure 3: Root Locus of PI controller.

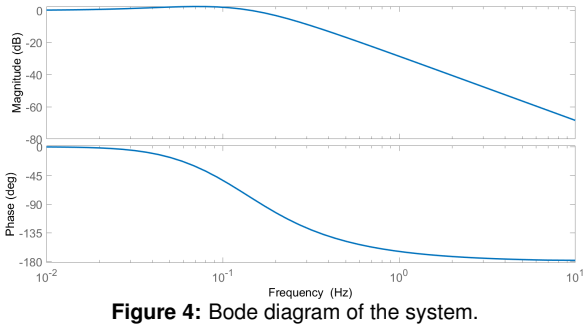

Figure 4: Bode diagram of the system.

3.4. Lower Level Controller

In the lower controller, the throttle input is calculated so as to track the desired acceleration determined by the upper controller. This simplified model is typically based on the assumptions that the torque converter in the vehicle is locked and that there is zero-slip between the tires and the road.

3.4.1 Engine Torque Calculation

We start by considering the case that the torque converter is locked ($T_t = T_p$), the car isn't undergoing a gear shift and the longitudinal tire slip is negligible. To this effect, the wheel speed ω_w is proportional to the engine speed ω_e and related through the gear ratio R as

$$\omega_w = R\omega_e \quad (23)$$

and the transmission shaft speed, ω_t, is equal to the engine speed. The longitudinal vehicle velocity is approximated by $\dot{x} = r_{eff}\omega_w$ and therefore the longitudinal acceleration is

$$\ddot{x} = r_{eff} R \dot{\omega}_e \quad (24)$$

So the longitudinal vehicle equation is

$$m\dot{x} = F_x - R_x - F_{aero} \quad (25)$$

with F_x being the total longitudinal tire force from all tires, R_x is the rolling resistance force and F_{aero} is the aerodynamic drag force. Using the previous equation, this can be rewritten as

$$F_x = mRr_{eff}\dot{\omega}_e + R_x + F_{aero} \tag{26}$$

Using the equation for wheel dynamics, we can obtain the torque at the wheels required to produce the desired acceleration

$$T_{wheel} = I_w R\dot{\omega}_e + mRr_{eff}^2\dot{\omega}_E + r_{eff}F_{aero} + r_{eff}R_x \tag{27}$$

Then, using the equation for transmission dynamics

$$\tau\dot{T}_{wheel} + T_{wheel} = \frac{1}{R}T_t \tag{28}$$

and considering that $\omega_t = \omega_e$ and $T_t = T_p$, we get

$$\begin{cases} T_p = (I_t + I_w R^2 + mR^2 r_{eff}^2)\dot{\omega}_e + \\ Rr_{eff}F_{aero} + Rr_{eff}R_x \end{cases} \tag{29}$$

for the pump torque load.

Using the equation for the engine rotational dynamics

$$I_e\dot{\omega}_e = T_i - T_f - T_a - T_p \tag{30}$$

We obtain

$$\begin{cases} I_e\dot{\omega}_e = T_{net} - (I_t + I_w R^2 + mR^2 r_{eff}^2)\dot{\omega}_e \\ -Rr_{eff}F_{aero} - Rr_{eff}R_x \end{cases} \tag{31}$$

Then if we consider $J_e = I_e + I_t + R^2 I_w + mR^2 r_{eff}^2$, the effective inertia reflected on the engine side, we can define

$$J_e\dot{\omega}_e = T_{net} - Rr_{eff}F_{aero} - Rr_{eff}R_x \tag{32}$$

If we substitute F_{aero} as $c_a(r_{eff}R\omega_e)^2$, the relation between ω_e and T_{net} can be modeled by

$$\dot{\omega}_e = \frac{T_{net} - c_a R^3 r_{eff}^3 \omega_e^2 - R(r_{eff}R_x)}{J_e} \tag{33}$$

Finally, we can conclude that if the net combustion torque is

$$T_{net} = \frac{J_e}{Rr_{eff}}\ddot{x}_{des} + [c_a R^3 r_{eff}^3 \omega_e^2 + R(r_{eff}R_x)] \tag{34}$$

then the acceleration of the car is equal to the desired acceleration defined by the upper-level controller, so $\ddot{x} = \ddot{x}_{des}$

4. Results and Simulations

4.1. Parameters

All the performed simulations are available at https://github.com/jmrsf1/car-longitudinal-control. The parameters used in the simulation, assuming the commonly used standard conditions of $15°C$, a barometric pressure of 101.32 kPa, rolling resistance coefficient of 0.015, typical for passenger cars with radial tires [6], are

- $A_F = 1.6 + 0.00056(m - 765)$=1.7316
- $h_{aero} = h = 0.5840\ m$
- $\rho = 1.225\ kg/m^3$
- $m = 1000\ kg$
- $f = 0.015$
- $C_{\sigma f} = C_{\sigma_r} = 40\ kN$
- V_{wind} =5.5 m/s
- $r_{eff} = 0.3534\ m$
- $l_r = 0.6\ m$
- $l_f = 0.74\ m$

4.2. Simulations

4.2.1 Car Model

The first experimented setup does not account for any driveline dynamics, which means the inputs of the system are the front and rear wheels velocity, ω_w, where it was assumed $\omega_{wf} = \omega_{wr}$.

Figures 5 and 6 show the behaviour of the car for constant ($\omega_w = 5.8\ rad/s$) and sinusoidal (with $25\ rad/s$ of amplitude and bias of $26\ rad/s$) input signals. In both experiments, the initial transient was ignored.

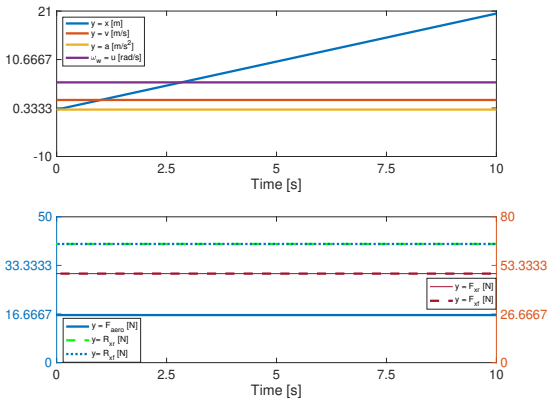

Figure 5: Behaviour and resulting forces of car model given constant input signal [Note: $R_{xr} = R_{xf}$ and $F_{xr} = Fxf$].

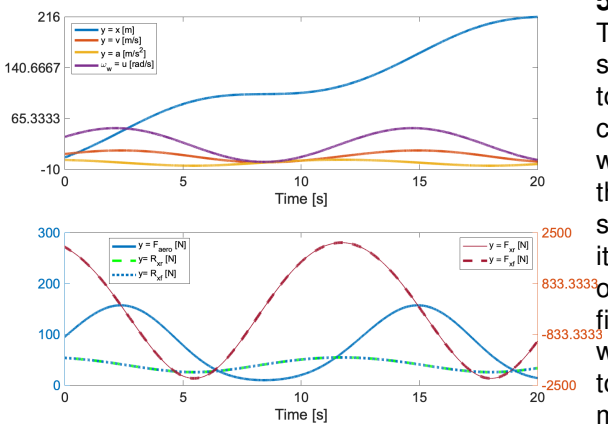

Figure 6: Behaviour and resulting forces of car model given sinusoidal input signal [Note: $R_{xr} = R_{xf}$ and $F_{xr} = Fxf$].

Both experiments show expected behavior: null acceleration for constant input and sinusoidal acceleration for the second experiment, which reinforces that the model was simulated correctly. Although many times not accounted for, we can see in Figures 5 and 6 that the forces that oppose movement (wind and rolling) are actually quite considerable, whose values can range from 15%-35% depending on how fast the car is traveling, as illustrated in 7.

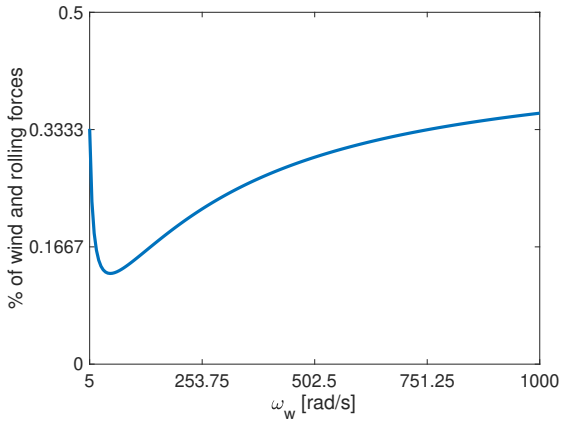

Figure 7: Percentage of negative acting forces as a function of front tire speed.

4.2.2 Driveline Dynamics

The simulation of driveline dynamics were not carried out due to the lack of an engine model. These models are very complex and their simulation would require a paper of its own. A possible alternative would be to use an engine map, *i.e.*, replace engine model with a map obtained from experimental data: $T_e(\omega_e, p_{man})$, where p_{man} is the engine's manifold pressure. Both alternative are not publicly available and easily obtainable.

5. Future Work

The modelling work presented in the paper is a small component in the development of an autonomous car. It is still necessary to add, and control, lateral dynamics by modelling a steering wheel and studying lateral movement, as well as the engine. After that sensor integration should be studied such as GPS for position, IMU for velocity and LiDAR for obstacle detection, with the help of a state estimator such as the extended kalman filter algorithm. All of this should be optimized towards a given energy budget. The final step would to design a physical model of the car that joins all mentioned components.

6. Conclusions

The paper has a clear objective of thoroughly studying longitudinal dynamics of a car as well as propose algorithms to control it. This work should serve as an important piece and/or starting step to incorporate in any work done in autonomous vehicle development.

References

[1] Rajesh Rajamani. *Vehicle Dynamics and Control*. Springer Science, New York, 2006.

[2] H. H. Korst and R. A. White. Coastdown tests: Determining road loads versus drag component evaluation. *SAE Transactions*, 99:1608–1614, 1990.

[3] Allan J. Kotwicki. Dynamic models for torque converter equipped vehicles. 1982.

[4] Dong-Il "Dan" Cho and J. Karl Hedrick. Automotive powertrain modeling for control. *Journal of Dynamic Systems Measurement and Control-transactions of The Asme*, 111:568–576, 1989.

[5] Pat Harrington et al. National transportation statistics (nts): Annual report, 1992. Technical report, United States. Dept. of Transportation. Research and Special Programs . . . , 1992.

[6] J.Y. Wong. *Theory of Ground Vehicles*. John Wiley & Sons,, 2001.